

Detection of SFBC-OFDM Signals in Frequency- and Time-Selective MIMO Channels

D. Sreedhar and A. Chockalingam

Department of ECE, Indian Institute of Science, Bangalore 560012, INDIA

Abstract— Use of space-frequency block coded (SFBC) OFDM signals is advantageous in high-mobility broadband wireless access, where the channel is highly time- as well as frequency-selective because of which the receiver experiences both inter-symbol interference (ISI) as well as inter-carrier interference (ICI). ISI occurs due to the violation of the ‘quasi-static’ fading assumption caused due to frequency- and/or time-selectivity of the channel. In addition, ICI occurs due to time-selectivity of the channel which results in loss of orthogonality among the subcarriers. In this paper, we are concerned with the detection of SFBC-OFDM signals on time- and frequency-selective MIMO channels. Specifically, we propose and evaluate the performance of an interference cancelling receiver for SFBC-OFDM which alleviates the effects of ISI and ICI in highly time- and frequency-selective channels.

I. INTRODUCTION

Multiple input multiple output (MIMO) orthogonal frequency division multiplexing (OFDM) techniques have become popular in modern wireless communication systems [1]. Space-time coding is a well known means of achieving improved performance in fading, in the form of transmit diversity using multiple transmit antennas [2]-[4]. Combining the advantages of space-time coding and OFDM is attractive in wireless system designs [1],[5]-[11]. This involves coding across space and frequency, which is often referred to as space-frequency coding (SFC). A way to do space-frequency coding is to take the space-time codes (e.g., Alamouti code), and apply them in the frequency dimension instead of time dimension [6]. That is, instead of mounting the space-time coded symbols on multiple time slots, they are mounted on multiple OFDM subcarriers. Use of orthogonal space-time block codes (OSTBCs) in the frequency dimension is attractive for SFC OFDM because of their low complexity decoding (i.e., single symbol decodability) and suitability for fast fading channels [1]. A space-frequency block coded (SFBC) OFDM using Alamouti code in the frequency dimension is defined in [12] for high mobility broadband wireless access.

For the time dimension OSTBCs to be single symbol decodable, the often made ‘quasi-static’ (QS) assumption (i.e., fade remains constant over one block time, which is valid only for slow fading channels, e.g., low/no mobility scenarios) is essential, the violation of which results in an error-floor. Rapid time-variations in the fading process result in such a violation. In SFBC OFDM systems, on the other hand, the QS assumption gets violated in the frequency dimension in highly frequency-selective channels (i.e., different subcarriers, and hence symbols belonging to the same SFBC block mounted on different subcarriers, see different channel gains), even if

time-variations in the fading process is very slow. The severity of this effect depends on the channel length L , power delay profile of the channel, and the SFBC block size. In highly frequency-selective channels (i.e., large L), this QS assumption violation becomes a source of significant inter-symbol interference (ISI) in the frequency dimension in SFBC OFDM. If left uncared for, this results in error floors [9]. Further, in any OFDM system, the orthogonality among subcarriers is lost if the channel changes within an OFDM symbol duration, which results in inter-carrier interference (ICI) [13]. Thus, in addition to the issue of ISI caused due to frequency-selectivity of the channel, SFBC OFDM experiences ICI caused due to time-selectivity of the channel (i.e., channel varying within one OFDM symbol duration) [14]. Like ISI, ICI, if uncared for, also will result in error floors.

Attempts have been made in the literature to cancel ICI in MIMO OFDM systems. Stamoulis *et al.*, in [14], have designed ICI-mitigating block linear filters for STBC-OFDM. However, they do not consider the loss of QS assumption in large delay spread channels. Improvement in performance is possible in SFBC-OFDM if both ISI (due to loss of QS assumption) as well as ICI (due to time-selectivity) can be estimated and cancelled. Linear detectors including zero-forcing and MMSE detectors can be used, which require inverse of matrices, the complexity of which can be alleviated if parallel interference cancellers (PIC) are employed for the purpose. Accordingly, in this paper, we propose a linear PIC approach to mitigate the effects of both ISI and ICI in SFBC-OFDM. The proposed detector estimates (using soft values of the demodulator output) and cancels the ISI in the first step, and then estimates and cancels the ICI in the second step. This two step procedure is then carried out in multiple cancellation stages. We evaluate the performance of the proposed detector for different codes including *i*) rate-1 Alamouti code [2], *ii*) rate-2/3 G_5 code [17], and *iii*) rate-3/5 G_6 code [17], for varying degrees of time-selectivity (different speeds) and frequency-selectivity (different channel lengths, L). We show that the proposed detector effectively cancels the ISI and ICI in high mobility, large delay spread channels.

The rest of the paper is organized as follows. In Sec. II, we present the SFBC-OFDM system model. In Sec. III, we present the proposed PIC detector. Results and discussions are presented in Sec. IV. Conclusions are given in Sec. V.

II. SYSTEM MODEL

We consider a MIMO OFDM system with N_c subcarriers, N_t transmit antennas, and N_r receive antennas. Let $X_k^{(i)}$ denote the complex data symbol transmitted on the k th subcarrier of an OFDM symbol from the i th transmit antenna. That is, the

This work was supported in part by the DRDO-IISc Program on Advanced Research in Mathematical Engineering.

symbols $\{X_k^{(i)}, k = 1, \dots, N_c, i = 1, \dots, N_t\}$ are transmitted in parallel on N_c subcarriers by N_t transmit antennas. After IDFT processing and insertion of guard interval of n_g samples at the transmitter, the discrete-time sequence at the i th transmit antenna is given by

$$x_n^{(i)} = \frac{1}{N_c} \sum_{k=0}^{N_c-1} X_{k+1}^{(i)} e^{j\frac{2\pi nk}{N_c}}, \quad -n_g \leq n \leq N_c - 1. \quad (1)$$

n_g is assumed to be longer than the maximum channel delay spread, L . Assuming perfect carrier synchronization, timing, and sampling at the receiver, the discrete-time received sequence at the j th receive antenna, $j = 1, 2, \dots, N_r$, can be written as

$$y_n^{(j)} = \sum_{i=1}^{N_t} \sum_{l=0}^{L-1} h^{(i,j)}(n; l) x_{n-l}^{(i)} + z_n^{(j)}, \quad j = 1, \dots, N_r, \quad -n_g \leq n \leq N_c - 1, \quad (2)$$

where $h^{(i,j)}(n; l)$ represents the discrete-time, time-varying (i.e., time-selective) L -length (i.e., frequency-selective) channel impulse response between the i th transmit and j th receive antennas, and $z_n^{(j)}$ is the additive noise on the j th receive antenna, assumed to be complex Gaussian with zero mean and variance N_0 .

After guard interval removal and DFT operation, the received signal on the k th subcarrier on the j th receive antenna, $Y_k^{(j)}$, can be written as

$$Y_k^{(j)} = \sum_{i=1}^{N_t} G_{k,k}^{(i,j)} X_k^{(i)} + \underbrace{\sum_{i=1}^{N_t} \sum_{m=0, m \neq k}^{N_c-1} G_{k,m}^{(i,j)} X_m^{(i)}}_{\text{ICI}} + Z_k^{(j)}, \quad (3)$$

where the coefficients $G_{k,m}^{(i,j)}$ are given by

$$G_{k,m}^{(i,j)} = \frac{1}{N_c} \sum_{n=0}^{N_c-1} \sum_{l=0}^{L-1} h^{(i,j)}(n; l) e^{j\frac{2\pi n(m-k)}{N_c}} e^{-j\frac{2\pi ml}{N_c}}. \quad (4)$$

Note that $G_{k,m}^{(i,j)}$, $k \neq m$ denotes the amount of carrier leak from m th subcarrier to the k th subcarrier, which essentially contributes to the ICI term in (3). It is easy to see that if the channel is not time-selective (i.e., time-flat) between all transmit/receive antenna pairs, i.e., if,

$$h^{(i,j)}(n_1; l) = h^{(i,j)}(n_2; l), \quad \forall i, j, l, \quad -n_g \leq n_1, n_2 < N_c - 1, \quad (5)$$

then $G_{k,m}^{(i,j)} = 0$ for $k \neq m$, and (3) reduces to (resulting in no ICI term)

$$Y_k^{(j)} = \sum_{i=1}^{N_t} \tilde{G}_{k,k}^{(i,j)} X_k^{(i)} + Z_k^{(j)}, \quad (6)$$

where $\tilde{G}_{k,k}^{(i,j)}$ is $G_{k,k}^{(i,j)}$ for time-flat channels, given by

$$\tilde{G}_{k,k}^{(i,j)} = \frac{1}{N_c} \sum_{l=0}^{L-1} h^{(i,j)}(n_1; l) e^{-j\frac{2\pi kl}{N_c}}. \quad (7)$$

A. Space-Frequency Block Coded OFDM

Here, we adopt the above system model to the case of space-frequency coded symbols transmission on different transmit antennas (space) and different subcarriers (frequency). That is, $X_k^{(i)}$'s are obtained from the output of the space-frequency coding scheme employed. Specifically, we consider the use of OSTBCs as the space-frequency codes. Let K denote the length of one space-frequency code block. We group the N_c subcarriers into N_g groups each having K subcarriers so that $N_c = N_g K + \kappa$ and each group carries one SFC block. For example, $K = 2$ for Alamouti code, and $K = 8$ for the G_3 code (rate-1/2, 3-transmit antenna OSTBC). If N_c is not a multiple of K , then there will not be any transmission on κ subcarriers, or, alternatively, these κ subcarriers can be used for pilot transmission.

Based on the above, the transmission of a SFBC OFDM frame can be written as an $N_c \times N_t$ matrix

$$\mathbf{X} = \begin{bmatrix} X_1^{(1)} & \dots & X_1^{(N_t)} \\ X_2^{(1)} & \dots & X_2^{(N_t)} \\ \vdots & \vdots & \vdots \\ X_{N_c}^{(1)} & \dots & X_{N_c}^{(N_t)} \end{bmatrix} = \begin{bmatrix} \mathbf{X}(1) \\ \vdots \\ \mathbf{X}(N_g) \\ \mathbf{0}^{\kappa \times N_t} \end{bmatrix} \quad (8)$$

where $\mathbf{X}(q)$ is a $K \times N_t$ matrix, $q = 1, 2, \dots, N_g$. $\mathbf{X}(q)$ is from a OSTBC in P complex information symbols $[v_1(q), v_2(q), \dots, v_P(q)]$ and rate- P/K . The i th column of \mathbf{X} is transmitted on the i th transmit antenna after IDFT processing. For example, for SFBC OFDM with $N_c = 4$ using Alamouti code, $N_t = 2$ and the matrix \mathbf{X} can be written as

$$\mathbf{X}_{\text{Alamouti}} = \begin{bmatrix} v_1(1) & v_2(1) \\ -v_2(1)^* & v_1(1)^* \\ v_1(2) & v_2(2) \\ -v_2(2)^* & v_1(2)^* \end{bmatrix}. \quad (9)$$

Now, we stack all the K rows of $\mathbf{X}(q)$ into one $KN_t \times 1$ vector, $\bar{\mathbf{X}}(q)$. This $\bar{\mathbf{X}}(q)$ vector can be written as

$$\bar{\mathbf{X}}(q) = \mathbf{A}\mathbf{V}(q), \quad (10)$$

where $\mathbf{V}(q)$ is a $2P \times 1$ vector, given by

$$\mathbf{V}(q) = [v_{1I}(q), \dots, v_{PI}(q), v_{1Q}(q), \dots, v_{PQ}(q)], \quad (11)$$

where $v_{pI}(q)$ and $v_{pQ}(q)$, respectively, are the real and imaginary parts of the p th complex information symbol in the q th group, $p = 1, 2, \dots, P$, $q = 1, 2, \dots, N_g$. The matrix \mathbf{A} in (10) is a $KN_t \times 2P$ complex matrix which performs the coding on $\mathbf{V}(q)$. Again, for the SFBC OFDM with Alamouti code example, \mathbf{A} is given by

$$\mathbf{A}_{\text{Alamouti}} = \begin{bmatrix} 1 & 0 & j & 0 \\ 0 & 1 & 0 & j \\ 0 & -1 & 0 & -j \\ 1 & 0 & -j & 0 \end{bmatrix}. \quad (12)$$

Using (12) in (10), we get

$$\bar{\mathbf{X}}_{\text{Alamouti}}(q) = [v_1(q), v_2(q), -v_2(q)^*, v_1(q)^*]^T, \quad (13)$$

and

$$\mathbf{X}_{\text{Alamouti}}(q) = \begin{bmatrix} v_1(q) & v_2(q) \\ -v_2(q)^* & v_1(q)^* \end{bmatrix}. \quad (14)$$

B. Received Signal Model for SFBC OFDM

At the receiver, the DFT outputs, $Y_k^{(j)}$'s, of (3) are stacked to form a $KN_r \times 1$ vector for each group, as

$$\mathbf{Y}(q) = \left[Y_{r+1}^{(1)}, \dots, Y_{r+1}^{(N_r)}, \dots, Y_{r+K}^{(1)}, \dots, Y_{r+K}^{(N_r)} \right]^T, \quad (15)$$

where $r = (q-1)K$. Now, $\mathbf{Y}(q)$ in (15) can be written in the form

$$\mathbf{Y}(q) = \bar{\mathbf{H}}(q)\bar{\mathbf{X}}(q) + \mathbf{I}(q) + \mathbf{Z}(q), \quad (16)$$

where $\bar{\mathbf{H}}(q)$ is a $KN_r \times KN_t$ block diagonal matrix, given by

$$\bar{\mathbf{H}}(q) = \begin{bmatrix} \mathbf{H}(q,1) & \cdots & \mathbf{0} \\ \vdots & \ddots & \vdots \\ \mathbf{0} & \cdots & \mathbf{H}(q,K) \end{bmatrix}, \quad (17)$$

where $\mathbf{H}(q,s)$ is the $N_r \times N_t$ channel matrix, $q = 1, 2, \dots, N_g$, $s = 1, 2, \dots, K$, given by

$$\mathbf{H}(q,s) = \begin{bmatrix} G_{u,u}^{(1,1)} & \cdots & G_{u,u}^{(1,N_t)} \\ \vdots & \ddots & \vdots \\ G_{u,u}^{(N_r,1)} & \cdots & G_{u,u}^{(N_r,N_t)} \end{bmatrix}, \quad (18)$$

where $u = (q-1)K + s$. The noise vector $\mathbf{Z}(q)$ in (16) is given by

$$\mathbf{Z}(q) = \left[Z_{r+1}^{(1)}, \dots, Z_{r+1}^{(N_r)}, \dots, Z_{r+K}^{(1)}, \dots, Z_{r+K}^{(N_r)} \right]^T, \quad (19)$$

where $r = (q-1)K$. The interference vector $\mathbf{I}(q)$ in (16) can be written in the form

$$\mathbf{I}(q) = \bar{\mathbf{R}}(q)\bar{\mathbf{X}}(q) + \sum_{b=1, b \neq q}^{N_g} \bar{\mathbf{Q}}(q,b)\bar{\mathbf{X}}(b), \quad (20)$$

where the block matrices $\bar{\mathbf{R}}(q)$ and $\bar{\mathbf{Q}}(q,b)$ are given by

$$\bar{\mathbf{R}}(q) = \begin{bmatrix} \mathbf{0} & \mathbf{R}_{q'+1, q'+2} & \cdots & \mathbf{R}_{q'+1, q'+K} \\ \mathbf{R}_{q'+2, q'+1} & \mathbf{0} & \cdots & \mathbf{R}_{q'+2, q'+K} \\ \vdots & \vdots & \ddots & \vdots \\ \mathbf{R}_{q'+K, q'+1} & \mathbf{R}_{q'+K, q'+2} & \cdots & \mathbf{0} \end{bmatrix}, \quad (21)$$

$$\bar{\mathbf{Q}}(q,b) = \begin{bmatrix} \mathbf{R}_{q'+1, b'+1} & \cdots & \mathbf{R}_{q'+1, b'+K} \\ \vdots & \ddots & \vdots \\ \mathbf{R}_{q'+K, b'+1} & \cdots & \mathbf{R}_{q'+K, b'+K} \end{bmatrix}, \quad (22)$$

where $q' = (q-1)K$, $b' = (b-1)K$, and

$$\mathbf{R}_{x,y} = \begin{bmatrix} G_{x+1, y+1}^{(1,1)} & \cdots & G_{x+1, y+K}^{(1,N_t)} \\ \vdots & \ddots & \vdots \\ G_{x+K, y+1}^{(N_r,1)} & \cdots & G_{x+K, y+K}^{(N_r,N_t)} \end{bmatrix}. \quad (23)$$

C. Detection of SFBC-OFDM

For the case of time-flat and frequency-flat conditions (i.e., no ISI and no ICI), the detector for OSTBCs presented in [16] for conventional space-time codes can be used for detecting

SFBC OFDM as follows. For the time-flat case, (16) can be written as

$$\mathbf{Y}(q) = \mathbf{H}_{eq}(q)\mathbf{V}(q) + \mathbf{Z}(q), \quad (24)$$

where $\mathbf{H}_{eq}(q)$ is a $KN_r \times 2P$ equivalent channel matrix for the q th group, given by

$$\mathbf{H}_{eq}(q) = \bar{\mathbf{H}}(q)\mathbf{A}. \quad (25)$$

For the frequency-flat case, the quasi-static assumption holds, i.e., in (17)

$$\mathbf{H}(q,1) = \mathbf{H}(q,2) = \cdots = \mathbf{H}(q,K), \quad \forall q. \quad (26)$$

Now, from [16], the optimal detector for SFBC OFDM under the above conditions can be shown to be of the form

$$\hat{\mathbf{Y}}(q) = \Re(\mathbf{H}_{eq}^*(q)\mathbf{Y}(q)), \quad (27)$$

where $\hat{\mathbf{Y}}(q)$ is a $2K \times 1$ vector containing the estimates of the real and imaginary parts of the complex information symbols in a stacked up fashion, which can be shown to be [16]

$$\begin{aligned} \hat{\mathbf{Y}}(q) &= \Re[\mathbf{H}_{eq}^*(q)\mathbf{H}_{eq}(q)]\mathbf{V}(q) + \Re[\mathbf{H}_{eq}^*(q)\mathbf{Z}(q)] \\ &= \mathbf{\Lambda}(q)\mathbf{V}(q) + \hat{\mathbf{Z}}(q), \end{aligned} \quad (28)$$

where $\mathbf{\Lambda}(q) = \Re[\mathbf{H}_{eq}^*(q)\mathbf{H}_{eq}(q)]$ is a diagonal matrix, and hence there will not be any inter-symbol interference. Furthermore, it can also be shown that under these conditions $\hat{\mathbf{Z}}(q) = \Re[\mathbf{H}_{eq}^*(q)\mathbf{Z}(q)]$ is white Gaussian. Hence, the Euclidean distance based symbol-by-symbol detection on $\hat{\mathbf{Y}}(q)$ is optimal.

On the other hand, for the case when the quasi-static assumption is violated (in this case due to frequency-selectivity of the channel), then $\mathbf{\Lambda}(q)$ is not diagonal. Hence, the detector in (27) results in an error floor. The optimum detector for this system would be a Maximum Likelihood (ML) detector in P variables which will have exponential receiver complexity. Moreover, if the channel is time-selective, then there would be inter-carrier interference (16) as well to handle.

We illustrate the effect of interferences due to time- and frequency selectivity of the channel in Fig. 1, where we plot the output SIR of SFBC-OFDM with Alamouti code ($N_t = 2$), as a function of user velocity and channel delay spread (L equal-power Rayleigh fading paths) for $N_c = 128$ subcarriers, $\Delta_f = 0.5$ KHz subcarrier spacing, $f_c = 2.5$ GHz carrier frequency, $N_r = 1$ receive antenna, and no noise. From Fig. 1, it can be seen that the SIR degrades for increasing user velocity and channel delay spread. Even when the user is static (i.e., velocity = 0 Km/h and hence time-flat fading), the SIR degrades significantly for increasing L (e.g., about 30 dB of SIR degradation from $L = 2$ to $L = 16$). Also, for a given L , increasing velocity degrades SIR (e.g., about 8 dB degradation from 0 to 60 Km/h for $L = 8$). We further observe that cancellation techniques can be employed to recover the performance loss due to time- and frequency-selectivity induced interferences, which is our focus in the following section.

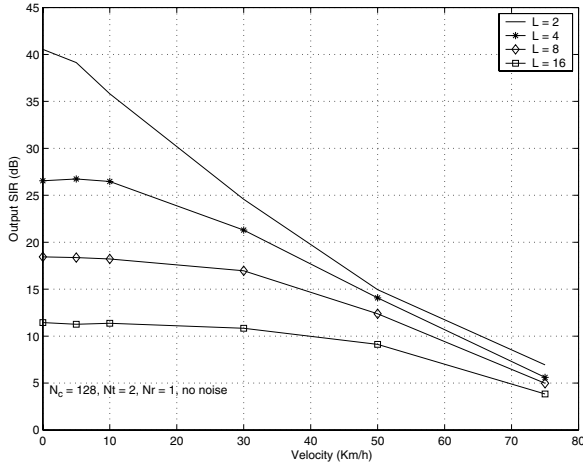


Fig. 1. Output SIR in SFBC-OFDM (without interference cancellation) as a function of user velocity and channel delay spread in time- and frequency-selective Rayleigh fading. $N_c = 128$, Alamouti code ($N_t = 2$), $N_r = 1$, $\Delta f = 0.5$ KHz, $f_c = 2.5$ GHz, no noise.

III. PROPOSED IC RECEIVER FOR SFBC OFDM

In this section, we propose a novel two-step PIC detector that cancels ISI and ICI in SFBC OFDM. The proposed detector estimates and cancels the ISI (caused due to the violation of the quasi-static assumption) in the first step, and then estimates and cancels the ICI (caused due to loss of subcarrier orthogonality) in the second step. This two step procedure is then carried out in multiple stages. The proposed detector is presented in the following.

We consider perfect channel knowledge at the receiver. Hence, in the notation, we will not differentiate between the actual channel and the channel estimate available at the receiver. The detector, however, can work with imperfect channel estimates.

First, we model the ISI caused by the violation of the quasi-static assumption. To do that, we split the block diagonal matrix $\bar{\mathbf{H}}(q)$ in (16) into two parts; *i*) a quasi-static part $\bar{\mathbf{H}}_{qs}(q)$, and *ii*) a non-quasi-static part $\bar{\mathbf{H}}_{nqs}(q)$, such that

$$\bar{\mathbf{H}}(q) = \bar{\mathbf{H}}_{qs}(q) + \bar{\mathbf{H}}_{nqs}(q), \quad (29)$$

where

$$\bar{\mathbf{H}}_{qs}(q) = \begin{bmatrix} \mathbf{H}(q, 1) & \mathbf{0} & \cdots & \mathbf{0} \\ \mathbf{0} & \mathbf{H}(q, 1) & \cdots & \mathbf{0} \\ \vdots & \vdots & \ddots & \vdots \\ \mathbf{0} & \mathbf{0} & \cdots & \mathbf{H}(q, 1) \end{bmatrix}, \quad (30)$$

and

$$\bar{\mathbf{H}}_{nqs}(q) = \begin{bmatrix} \mathbf{0} & \mathbf{0} & \cdots & \mathbf{0} \\ \mathbf{0} & \Delta\mathbf{H}(q, 2) & \cdots & \mathbf{0} \\ \vdots & \vdots & \ddots & \vdots \\ \mathbf{0} & \mathbf{0} & \cdots & \Delta\mathbf{H}(q, K) \end{bmatrix}, \quad (31)$$

where $\Delta\mathbf{H}(q, m) = \mathbf{H}(q, m) - \mathbf{H}(q, 1)$.

Similarly, we split the equivalent channel matrix $\mathbf{H}_{eq}(q)$, as

$$\mathbf{H}_{eq}(q) = \mathbf{H}_{eq-qs}(q) + \mathbf{H}_{eq-nqs}(q), \quad (32)$$

where $\mathbf{H}_{eq-qs}(q) = \bar{\mathbf{H}}_{qs}(q)\mathbf{A}$, and $\mathbf{H}_{eq-nqs}(q) = \bar{\mathbf{H}}_{nqs}(q)\mathbf{A}$.

Based on the above formulations and (20), we can write (16) as

$$\begin{aligned} \mathbf{Y}(q) &= \bar{\mathbf{H}}_{qs}(q)\bar{\mathbf{X}}(q) + \underbrace{\bar{\mathbf{H}}_{nqs}(q)\bar{\mathbf{X}}(q)}_{\text{QS violation}} \\ &+ \underbrace{\bar{\mathbf{R}}(q)\bar{\mathbf{X}}(q) + \sum_{b=1, b \neq q}^{N_g} \bar{\mathbf{Q}}(q, b)\bar{\mathbf{X}}(b)}_{\text{loss of orthogonality}} + \mathbf{Z}(q). \end{aligned} \quad (33)$$

As in (27), an estimate of $\mathbf{Y}(q)$ can be obtained as

$$\begin{aligned} \hat{\mathbf{Y}}(q) &= \Re(\mathbf{H}_{eq-qs}^*(q)\mathbf{Y}(q)) \\ &= \underbrace{\Re[\mathbf{H}_{eq-qs}^*(q)\mathbf{H}_{eq-qs}(q)]\mathbf{V}(q)}_{\text{desired signal}} \\ &+ \underbrace{\Re[\mathbf{H}_{eq-qs}^*(q)\mathbf{H}_{eq-nqs}(q)]\mathbf{V}(q)}_{\text{ISI}} \\ &+ \underbrace{\Re[\mathbf{H}_{eq-qs}^*(q)\bar{\mathbf{R}}(q)\bar{\mathbf{X}}(q)] + \Re[\mathbf{H}_{eq-qs}^*(q) \sum_{b=1, b \neq q}^{N_g} \bar{\mathbf{Q}}(q, b)\bar{\mathbf{X}}(q)]}_{\text{ICI}} \\ &+ \underbrace{\Re[\mathbf{H}_{eq-qs}^*(q)\mathbf{Z}(q)]}_{\text{noise}}. \end{aligned} \quad (34)$$

As can be seen, (34) identifies the desired signal, ISI, ICI, and noise components present in the estimate $\hat{\mathbf{Y}}(q)$. Based on this received signal model in (34) and the knowledge of the matrices $\mathbf{H}_{eq-qs}(q)$, $\mathbf{H}_{eq-nqs}(q)$, $\bar{\mathbf{R}}(q)$, $\bar{\mathbf{Q}}(q, b) \forall q, b$, we formulate the proposed interference estimation and cancellation procedure as follows.

- 1) For each SF code block q , estimate the information symbols $\hat{\mathbf{V}}(q)$ from (34), ignoring ISI and ICI.
- 2) For each SF code block q , obtain an estimate of the ISI (i.e., an estimate of the 2nd term in (34)) from the estimated symbols $\hat{\mathbf{V}}(q)$ in the previous step.
- 3) Cancel the estimated ISI from $\hat{\mathbf{Y}}(q)$.
- 4) Using $\hat{\mathbf{V}}(q)$ from step 1, regenerate $\hat{\bar{\mathbf{X}}}(q)$ using (10). Then, using $\hat{\bar{\mathbf{X}}}(q)$, obtain an estimate of the ICI (i.e., an estimate of the sum of 3rd and 4th terms in (34)).
- 5) Cancel the estimated ICI from the ISI cancelled output in step 3.
- 6) Take the ISI and ICI cancelled output from step 5 as the input back to step 1 (for the next stage of cancellation).

Based on the above, and defining $\Lambda(q) = \Re[\mathbf{H}_{eq-qs}^*(q)\mathbf{H}_{eq-qs}(q)]$, the cancellation algorithm for the m th stage can be summarized as follows.

Initialization : Set $m = 1$.

Evaluate

$$\hat{\mathbf{Y}}^{(m)}(q) = \Re(\mathbf{H}_{eq-qs}^* \mathbf{Y}(q)), \quad 1 \leq q \leq N_g. \quad (35)$$

Loop

Estimate

$$\hat{\mathbf{V}}^{(m)}(q) = \hat{\mathbf{Y}}^{(m)}(q)\Lambda^{-1}(q), \quad 1 \leq q \leq N_g. \quad (36)$$

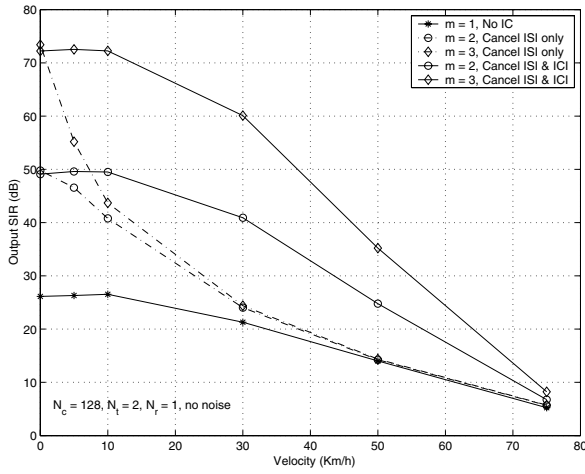


Fig. 2. Output SIR in SFBC-OFDM (with interference cancellation) as a function of user velocity in time- and frequency-selective Rayleigh fading for $L = 4$. $N_c = 128$, Alamouti code ($N_t = 2$), $N_r = 1$, $\Delta_f = 0.5$ KHz, $f_c = 2.5$ GHz, no noise.

Cancel ISI

$$\hat{\mathbf{Y}}^{(m+1)}(q) = \hat{\mathbf{Y}}^{(1)}(q) - \Re(\mathbf{H}_{eq-qs}^*(q)\mathbf{H}_{eq-nqs}(q))\hat{\mathbf{V}}^{(m)}(q), \quad 1 \leq q \leq N_g. \quad (37)$$

Form $\hat{\mathbf{X}}^{(m)}(q)$ from,

$$\hat{\mathbf{X}}^{(m)}(q) = \mathbf{A}\hat{\mathbf{V}}^{(m)}(q), \quad 1 \leq q \leq N_g. \quad (38)$$

Cancel ICI

$$\hat{\mathbf{Y}}^{(m+1)}(q) = \hat{\mathbf{Y}}^{(m+1)}(q) - \Re\left(\mathbf{H}_{eq-qs}^*(q)\bar{\mathbf{R}}(q)\hat{\mathbf{X}}^{(m)}(q)\right) - \Re\left(\mathbf{H}_{eq-qs}^*(q)\sum_{b=1, j \neq q}^{N_g}\bar{\mathbf{Q}}(q, b)\hat{\mathbf{X}}^{(m)}(b)\right), \quad 1 \leq q \leq N_g. \quad (39)$$

$$m = m + 1$$

goto Loop.

It is noted that the above cancellation algorithm has polynomial complexity. Also, since $\mathbf{\Lambda}(q) = \Re(\mathbf{H}_{eq-qs}^*\mathbf{H}_{eq-qs})$ is a diagonal matrix, its inversion is simple. In practice, accurate estimation of the channel coefficients is essential, which can be achieved, for example, using the algorithm proposed in [14].

IV. SIMULATION RESULTS

We evaluated the SIR and BER performance of the proposed interference cancelling detector through simulations. First, in Fig. 2, we illustrate the improvement in output SIR achieved using the proposed IC detector for the same system parameters used in Fig. 1 (for the case of $L = 4$). We consider two cases, where the detector cancels *i*) only ISI (bypassing the ICI cancellation part in the algorithm), and *ii*) both ISI and ICI. Plots for no cancellation ($m = 1$) as well as 2nd and 3rd stages of cancellation ($m = 2, 3$) are shown. From Fig. 2, we observe that in time-flat channels (velocity = 0 Km/h), cancellation of ISI only improves performance significantly, and

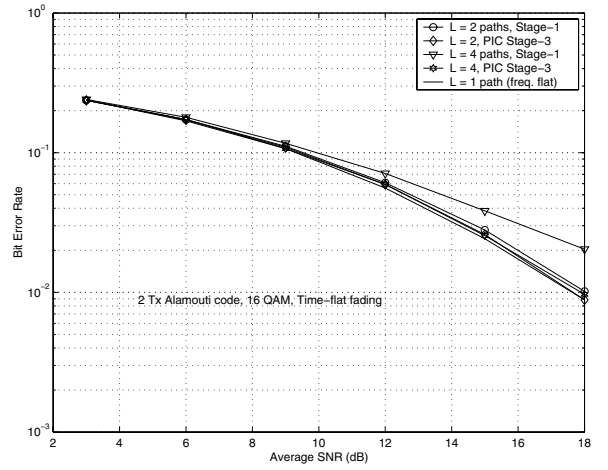


Fig. 3. BER performance as a function of SNR for space-frequency coded OFDM on time-flat and frequency-selective fading. $N_c = 64$, $N_r = 1$, Alamouti code ($N_t = 2$), 16-QAM, $L = 2$ and $L = 4$.

cancelling ICI also in this case does not bring additional benefits. However, for non-zero user velocities, cancellation of ISI only is not adequate, and there is substantial further improvement that is possible by the cancellation of ICI as well. For example, at a speed of 30 Km/h, canceling only the ISI improves the SIR by just about 4 dB compared to no cancellation, whereas canceling both ISI and ICI improves the SIR by about 20 dB for $m = 2$ and 40 dB for $m = 3$. This illustrates the potential for significant improvement of using the proposed joint cancellation of both ISI and ICI.

In Fig. 3, we plot the BER performance of the PIC detector in time-flat (velocity = 0 Km/h) and frequency-selective Rayleigh fading with $L = 2$ and $L = 4$ equal power paths for SFBC OFDM using Alamouti code and 16-QAM. The other system parameters used are $N_c = 128$, $N_r = 1$, $\Delta_f = 312.5$ KHz, and $f_c = 5.4$ GHz. In Fig. 3, Stage-1 performance corresponds to the case of no cancellation, whereas Stage-3 performance is after two stages of proposed cancellation. For comparison purposes, we have also plotted the performance for time-flat and frequency-flat fading (i.e., no ISI and no ICI), which provides the best possible performance. From Fig. 3, it can be observed that for $L = 2$ (i.e., channel delay spread is small), the ISI induced is small, and hence there is no major performance improvement due to the cancellation. However, for $L = 4$ (i.e., delay spread of the channel is large), the ISI induced is high, and, in this case, the proposed cancellation results in significant performance gain (e.g., about 2 dB gain at 2×10^{-2} BER).

In Fig. 4, we plot the BER performance of SFBC OFDM on time-selective and frequency-selective fading for rate-2/3 G_5 OSTBC (5 Tx antennas) using 16-QAM. The mobile speed is 50 Km/h and $L = 2$. The BER plot for the case of time-flat and frequency-flat fading (i.e., the case of no ISI and no ICI) is also plotted for comparison. From Fig. 4, it can be seen that due to ISI and ICI the performance without cancellation (i.e., Stage-1) is severely affected compared to the case of time-flat and frequency-flat fading. However, the performance is significantly improved by the proposed PIC detector (Stage-2 and Stage-3) because of the effective mitigation of ISI and

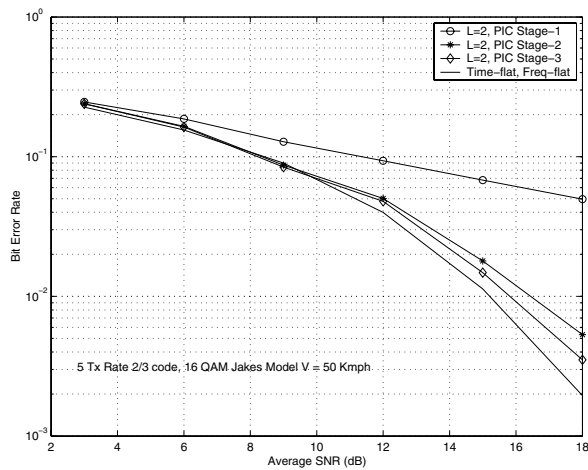


Fig. 4. BER performance as a function of SNR for space-frequency coded OFDM on time-selective and frequency-selective fading. $N_c = 64$, $N_r = 1$, 5-Tx antennas ($N_t = 5$), rate-2/3 G_5 code, 16-QAM, $L = 2$, and mobile speed = 50 Km/h.

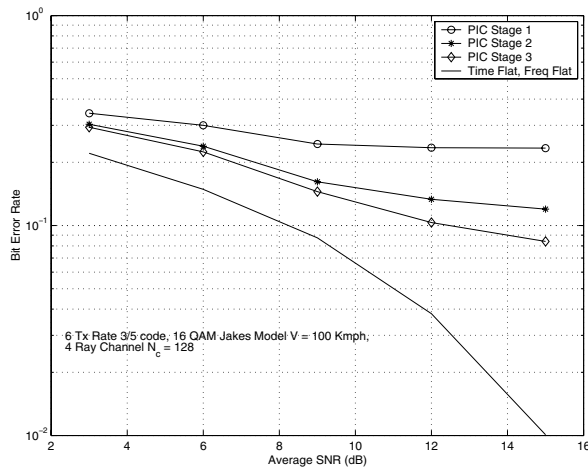


Fig. 5. BER performance as a function of SNR for space-frequency coded OFDM on time-selective and frequency-selective fading. $N_c = 128$, $N_r = 1$, 6-Tx antennas ($N_t = 6$), rate-3/5 G_6 code, 16-QAM, $L = 4$, and mobile speed = 100 Km/h.

ICI. For example, at a BER of 5×10^{-2} , the proposed canceller results in about 6 dB improvement in performance compared to the case of no cancellation at the receiver.

Finally, in Fig. 5, the BER performance of SFBC OFDM using rate-3/5 G_6 code and 16-QAM is presented. The user velocity is 100 Km/hr and $L = 4$ indicating a severe time-selective and frequency-selective channel scenario. It can be seen that while the no cancellation receiver (Stage 1) significantly loses performance compared to the time-flat and frequency-flat performance, the proposed two-step PIC is found to improve performance by effectively cancelling the ISI and ICI.

V. CONCLUSIONS

We presented a PIC algorithm for cancelling frequency-selectivity induced ISI and time-selectivity induced ICI in SFBC OFDM systems. In the first step of the algorithm, an estimate of ISI is obtained and cancelled, and in the second step an estimate of the ICI is obtained and cancelled. This two-step

procedure is repeated in multiple stages to reduce the ISI-ICI induced error-floors. Our simulation results for varying degrees of time- and frequency-selectivity of the channel show that the proposed detector effectively mitigates the effects of ISI and ICI. The proposed PIC detector algorithm can be easily extended to space-time-frequency (STFC) coded OFDM as well.

REFERENCES

- [1] H. Yang, "A road to future broadband wireless access: MIMO-OFDM-based air interface," *IEEE Commun. Mag.*, pp. 53-60, January 2005.
- [2] S. M. Alamouti, "A simple transmit diversity technique for Wireless communications" *IEEE J. Select Areas Commun.*, vol. 16, pp. 1451-1458, October 1998.
- [3] V. Tarokh, H. Jafarkhani, and A. R. Calderbank, "Space-time block coding for wireless communications: Performance results," *IEEE J. Sel. Areas in Commun.*, vol. 17, no. 3, pp. 451-460, 1999.
- [4] V. Tarokh, H. Jafarkhani, and A. R. Calderbank, "Space-time block codes from orthogonal designs," in *IEEE Trans. Inform. Theory*, vol. 45, pp. 1456-1467, July 1999.
- [5] D. Agrawal, V. Tarokh, A. Naguib, and N. Seshadri, "Space-time coded OFDM high data-rate wireless communication over wideband channels," *Proc. IEEE VTC'98*, pp. 2232-2236, May 1998.
- [6] H. Bolcskei and A. Paulraj, "Space-frequency coded broadband OFDM systems," in *Proc. of IEEE WCNC'2000*, pp. 16, September 2000.
- [7] Z. Liu, Y. Xin, and G.B. Giannakis, "Space-time-frequency coded OFDM over frequency-selective fading channels," *IEEE Trans. on Signal Processing*, vol. 50, no. 10, pp. 2465-2476, October 2002.
- [8] Y. Gong, and K.B. Letaief, "An efficient space-frequency coded wideband OFDM system for wireless communications," *IEEE Trans. on Commun.*, vol.51, no. 12, pp. 2019-2029, December 2003.
- [9] K. Lee, and D. Williams, "A space-frequency transmitter diversity technique for OFDM systems," *Proc. IEEE GLOBECOM'2000*, vol.3, 2000.
- [10] G. Bauch, "Space-time block codes versus space-frequency block codes," *Proc. IEEE VTC'03*, pp. 567-571, 2003.
- [11] L. Shao and S. Roy, "Rate-one space frequency block codes with maximum diversity for MIMO-OFDM," *IEEE Trans. on Wireless Commun.*, vol. 4, no. 4, pp. 1674-1687, July 2005.
- [12] IEEE 802.20 - Working Group on High Mobility Broadband Wireless Access, 2005.
- [13] P. Robertson and S. Kaiser, "Analysis of the loss of orthogonality through Doppler spread in OFDM systems," *Proc. IEEE GLOBECOM'99*, pp. 701-706, 1999.
- [14] A. Stamoulis, S. N. Diggavi, and N. Al-Dhahir, "Inter-carrier interference in MIMO-OFDM," *IEEE Trans. on Signal Processing*, vol. 50, no. 10, pp. 2451- 2464, October 2002.
- [15] F. C. Zheng and A. G. Burr, "Signal detection for orthogonal space-time block coding over time-selective Fading channels: A PIC approach for the G_i systems," *IEEE Tran. on Commun.*, vol. 53, no. 6, pp. 969-972, June 2005.
- [16] A. Agrawal, G. Ginis, and J. M. Cioffi, "Channel diagonalization through orthogonal space-time coding," *Proc. IEEE ICC'2002*. 2002.
- [17] W. Su and X. G. Xia, and K. J. Ray Liu, "A systematic design of High-rate complex orthogonal space-time block codes" *IEEE Commun. Letters*, vol. 8, no.6, pp. 380-382, June 2004.